Heavy Quarks at HERA-B and Tevatron

Peter Krizan

University of Ljubljana, Slovenia

1 Introduction

The two lectures, that are written up in this paper, try to answer the questions why hadron machines look very promising in B physics studies, what are the problems in b hadron detection, and how these were solved in three experiments, CDF as an example of a collider experiment, a fixed target experiment HERA-B, and BTeV, a collider experiment in the forward direction.

Some of the advantages of hadron machines are evident from a comparison table, Tab.1. It then becomes clear that the $b\bar{b}$ production cross section is typically much higher in a hadron machine, as compared to e^+e^- machines. At HERA-B, where the cross-section is comparable to the e^+e^- production, the $b\bar{b}$ production rate can be made high by adjusting the luminosity.

An additional advantage of the b hadrons produced in hadronic collisions if compared to the B-factories at $\Upsilon(4s)$ is a large boost which results in a long average decay length, $< L > = < \beta\gamma >$ 480 μm. Finally, in addition to B^0 and $B^\pm$ mesons also other b hadrons, B_s, B_c, Λ_b, are produced.

However, when designing a detector for b hadrons at a hadron machine, we have to consider several issues. Since in most cases we are dealing with multiple interactions per event, the detector has to be able to tolerate high track densities (see Fig. 1). In addition, because of a rather low ratio of the signal cross section to the total cross section, high interaction rates are needed. These experimental conditions tell us that the employed detectors have to have a sufficiently fine granularity, and have to be radiation hard.

The low ratio of signal to total cross section also requires an early selection of interesting events. Therefore, highly selective triggers with high background suppression are needed. Two approaches are used in forming trigger decisions. The first relies on the fact that the decay products of a B meson have rather high transverse momenta in the case of few-body final states, as e.g. $B \to \mu\nu X$, $B \to J/\psi K_s \to \mu\mu\pi\pi$, $B \to \pi^+\pi^-$. In particular, the final states with leptons and lepton pairs are very attractive because their

Production	$e^+e^- \to \Upsilon(4s) \to B\bar{B}$	$e^+e^- \to Z^0 \to b\bar{b}$	$pA \to b\bar{b}X$	$p\bar{p} \to b\bar{b}X$	$p\bar{p}(p) \to b\bar{b}X$ forward
Accelerator	CESR, DORIS PEPII, KEKB	LEP, SLD	HERA p	Tevatron	Tevatron
Spectrometer	CLEO, ARGUS BaBar, BELLE	ALEPH, DELPHI, L3, OPAL, SLD	HERA-B	CDF, D0	BTeV
$\sigma(b\bar{b})$	≈ 1 nb	≈ 6 nb	≈ 12 nb	≈ 50 μb	≈ 100 μb
$\sigma(b\bar{b})$:$\sigma(had)$	0.26	0.22	10^{-6}	10^{-3}	$2 \cdot 10^{-3}$
B^0, B^+	yes	yes	yes	yes	yes
$B_s^0, B_c^+, \Lambda_b^0$	no	yes	yes	yes	yes
boost $< \beta\gamma >$	0.06 (0.5)	6	≈ 20	$\approx 2-4$	$\approx 4-20$
multiple events	no	no	yes, 4	yes	yes, 2
main trigger	inclusive	inclusive	lepton pairs	leptons	displaced vertex

Table 1. *Comparison of $b\bar{b}$ production at e^+e^- and hadron machines discussed in this paper.*

identification can be made rather quickly, on time scales of a few hundred ns.

Another triggering approach takes advantage of large displacements of decay vertices of b hadrons from the interaction point. In the case of HERA-B this amounts to typically 1 cm. Both approaches have been used in the experiments presented in this paper. Traditionally the detection of high p_T tracks is faster, and therefore used in the early trigger decision stage, while the reconstruction of vertex takes more time, and is a part of the higher trigger levels. As we shall see later, BTeV will be the first experiment to change this order.

In what follows, we shall first briefly review the excellent results from the CDF detector, that will serve as a proof of principle. We shall then discuss the HERA-B and BTeV experiments.

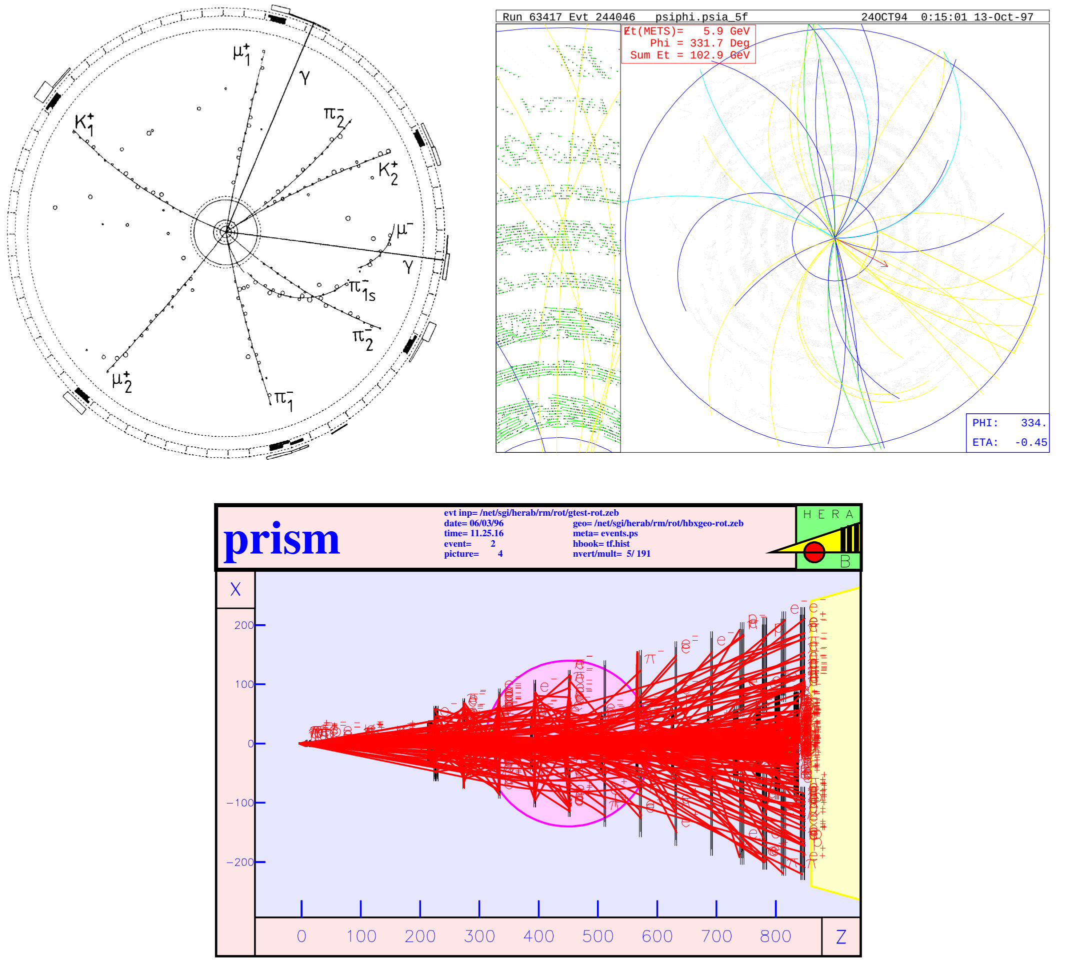

Figure 1. *Comparison of $b\bar{b}$ events at an e^+e^- machine (top left: ARGUS), an event recorded in the CDF spectrometer (top right), and a needle in a haystack, an example of a $b\bar{b}$ event at HERA-B.*

2 B physics with CDF

2.1 CDF spectrometer

The Tevatron collider provides $p\bar{p}$ collisions at a center-of-mass energy of 2 TeV in two interaction regions, for the two experiments, CDF and D0. The CDF detector (Abe 1988) is a general purpose magnetic spectrometer. It has a silicon microstrip vertex detector, a vertex TPC, a main tracking chamber, an electromagnetic and a hadronic calorimeter, and a system of muon chambers (Fig. 2).

For the b physics studies there are two interesting figures of merit illustrated in Fig. 5. The di-muon invariant mass resolution in the J/ψ region is 16 MeV. The resolution in the position of the vertex amounts to 40-50 μm for muon pairs from J/ψ decays. The performance of the vertex detector is essential for improving the signal to background ratio for b physics studies, as can be seen on the example of the $B_d \to J/\psi K^+$ decay channel in Fig. 3.

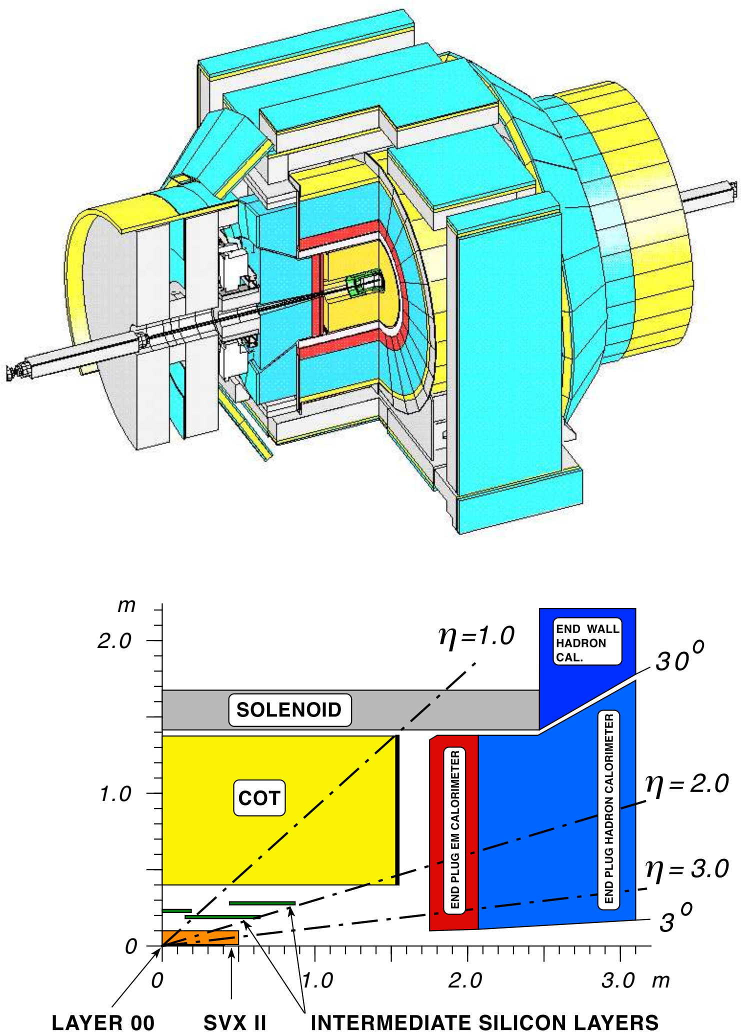

Figure 2. *CDF spectrometer: isometric view (top) with a vertex detector system, a central tracking chamber, electromagnetic and hadronic calorimeters, a superconducting solenoid, and muon chambers; side view after the upgrade (bottom) with silicon vertex detector including the additional layer (L00), silicon tracker, central tracking chamber (COT), and calorimeter.*

2.2 CDF results

Among the highlights of the results collected with the CDF spectrometer, we first note that the excellent performance of the vertex detector allows the time evolution related quantities, i.e. lifetimes and mixing, to be measured well. The results of lifetime measurements of b hadrons are summarized in Fig. 5, with resolutions similar to the ones measured in the LEP experiments. We also note, that the achieved precision of the B_d mixing measurements (Gay 2000) matches the precision of LEP experiments, as can be seen again from Fig. 5.

The measurement of B_s mixing as carried out with the CDF spectrometer resulted in a lower limit of $\Delta m_s > 5.8\mathrm{ps}^{-1}$ at 95% confidence level. Among the contributions to the spectroscopy of b hadrons the most important are the first observation of the B_c

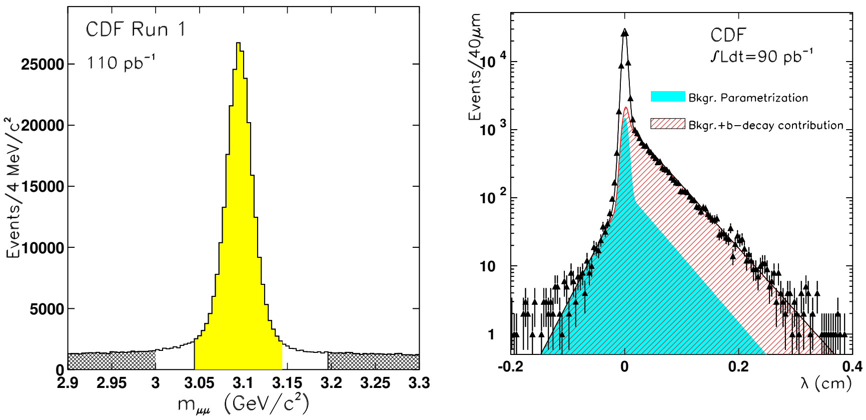

Figure 3. *Examples of CDF performance: distribution of di-muon invariant mass (left), decay length distribution for di-muon events from the J/ψ mass band (right).*

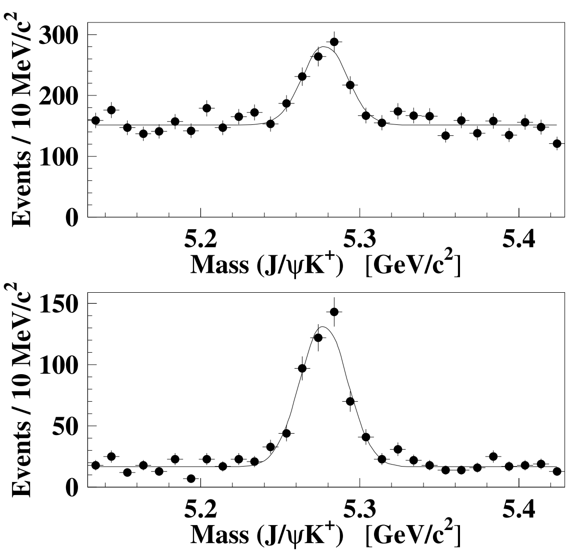

Figure 4. *Cleaning up the $J/\psi K^+$ signal: a cut on decay length ($> 100\mu m$) (bottom) significantly improves the signal to background ratio.*

meson and the determination of masses of B_s, Λ_b and B_c hadrons. The experiment also measured the cross section $\sigma(p\bar{p} \to bX)$ which turned out to be larger than theoretical predictions by about a factor of 2 (Bedeschi 2001).

CDF has also contributed the first estimate of one of the CP violation parameters in the B system, $\sin 2\beta = 0.79^{+0.41}_{-0.44}$ (Affolder 2000). For the next generation of precision b physics experiments a measurement of the polarization in the $B_s \to J/\psi\phi$ decay is of importance as an input for the measurement of $\Delta\Gamma/\Gamma$ (Affolder 2000a). Last but not least, CDF showed that at hadron machines also rare decays, as e.g. $B_d \to K^*\mu\mu$, can be studied (Affolder 1999). The interested reader should consult overview papers (Paulini 1999, Pitts 2000) for more details.

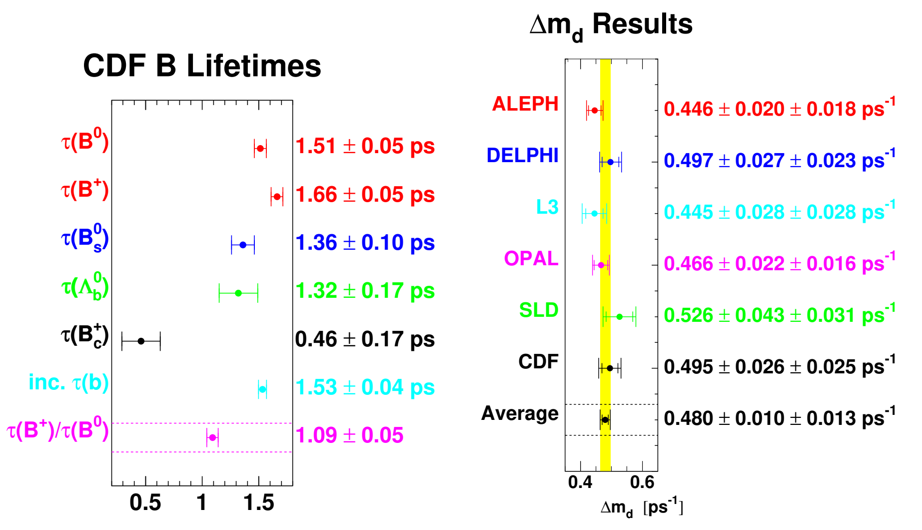

Figure 5. *Examples of measurements with the CDF spectrometer: lifetimes of b hadrons (left), and the B_d mixing parameter Δm_d compared to the results from LEP and SLC (right).*

2.3 CDF plans for future

The prospects of the CDF detector to contribute substantially in the next few year are founded on two developments. For the next running period (known as 'Run II') the Tevatron collider was upgraded, in particular its injector and the anti-proton source. The bunch spacing changed from 3.5 μs to 396 ns in the first step, and will be further reduced to 132 ns in the second stage. It is expected that 2 fb^{-1} of integrated luminosity will be accumulated during the first stage in the years 2001-04, and as much as 15 fb^{-1} in the second stage until 2007. Both numbers should be compared to the 0.1 fb^{-1} of data collected in the previous period, known as Run I.

A major upgrade of the CDF and D0 spectrometers was carried out to match the reduced bunch spacing and to further improve the performance of the spectrometer. The upgraded CDF detector, shown in Fig. 2, has an increased muon system and silicon detector solid angle coverage. It also has a new central tracker, a drift chamber and additional silicon layers between the silicon vertex detector and the drift chamber. A time-of-flight counter was added for a π/K separation up to 1.6 GeV/c. For a dramatic increase in the expected B_s mixing reach, the vertex resolution will be improved by an additional silicon layer close to the beam (see Appendix A for details on how to measure B_s mixing). Last but not least, the trigger system now includes a fast track search in the first level, and a silicon vertex tracking algorithm in the second level. This will allow to lower the p_t threshold for muons, as well as to define a two track trigger.

With the integrated luminosity of 2fb^{-1}, aimed for in the first period of Run II, the following measurements can be performed (Tanaka 2001). It is expected that the CP violation parameter $\sin 2\beta$ will be measured with an error of 0.043. B_s mixing observation will be possible up to $x_s = 60$ at 5σ significance. $\Delta\Gamma/\Gamma$ for B_s mesons will be measured with an 0.05 error through the decay channel $B_s \to J/\psi\phi$. It is also expected that the forward-backward asymmetry A_{FB} in the rare decay $B_d \to K^*\mu\mu$ will be measured. Finally, the $b\bar{b}$ production cross section section will be studied, as well as some exclusive decays of the B_c meson, $B_c \to J/\psi\ell\nu$ and $J/\psi\pi$.

3 HERA-B

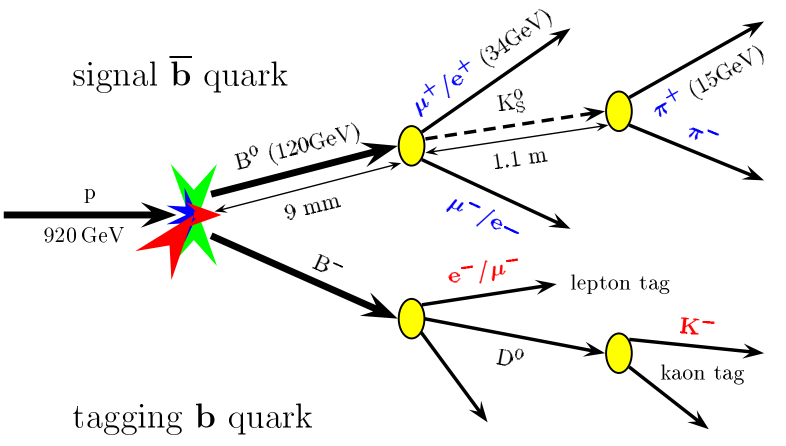

Figure 6. *A $B \to J/\psi K^0_S$ event with typical momenta and decay distances as expected in the HERA-B experiment.*

HERA-B is a fixed target experiment at the storage ring HERA at DESY. The experiment was originally designed (Lohse et al. 1994) for measuring CP violation in the decays of neutral B mesons to $J/\psi K^0_S$ (Fig. 6). Bottom hadrons at HERA-B are produced in reactions of 920 GeV protons from the storage ring with an internal wire target. The average momentum of the B is 120 GeV, so it travels about 1 cm before decay. The J/ψ from the decay $B^0 \to J/\psi K^0_S$ can be triggered and reconstructed in its dileptonic decay mode. From two existing measurements of $\sigma_{b\bar{b}}$ in the relevant kinematic region (Jansen et al. 1995, Alexopoulos et al. 1999), it follows that the fraction of events containing b quarks is of order of 10^{-6}. Also, the branching ratio for the decay $B^0 \to J/\psi K^0_S$ is small. Consequently, the ratio of the cross section for the reaction $B^0 \to J/\psi K^0_S \to l^+l^-\pi^+\pi^-$ and the inelastic cross section is of the order 10^{-11}. Accordingly, a very high interaction rate is necessary. At the HERA-B design interaction rate of 40 MHZ, four proton–nucleon interactions occur in average per bunch crossing (every 96 ns). This interaction rate leads to fluxes of charged particles through the detector components which can be compared with fluxes expected at LHC.

3.1 HERA-B spectrometer

HERA-B is a large magnetic forward spectrometer (Fig. 7) with outer dimension of 20 m $\times$ 9 m $\times$ 7 m. It covers a solid angle from 10 mrad polar angle with respect to the beam direction to about 200 mrad, corresponding to about 90% coverage in the center of mass system. The main detector components are wire targets, a vertex detector system, a

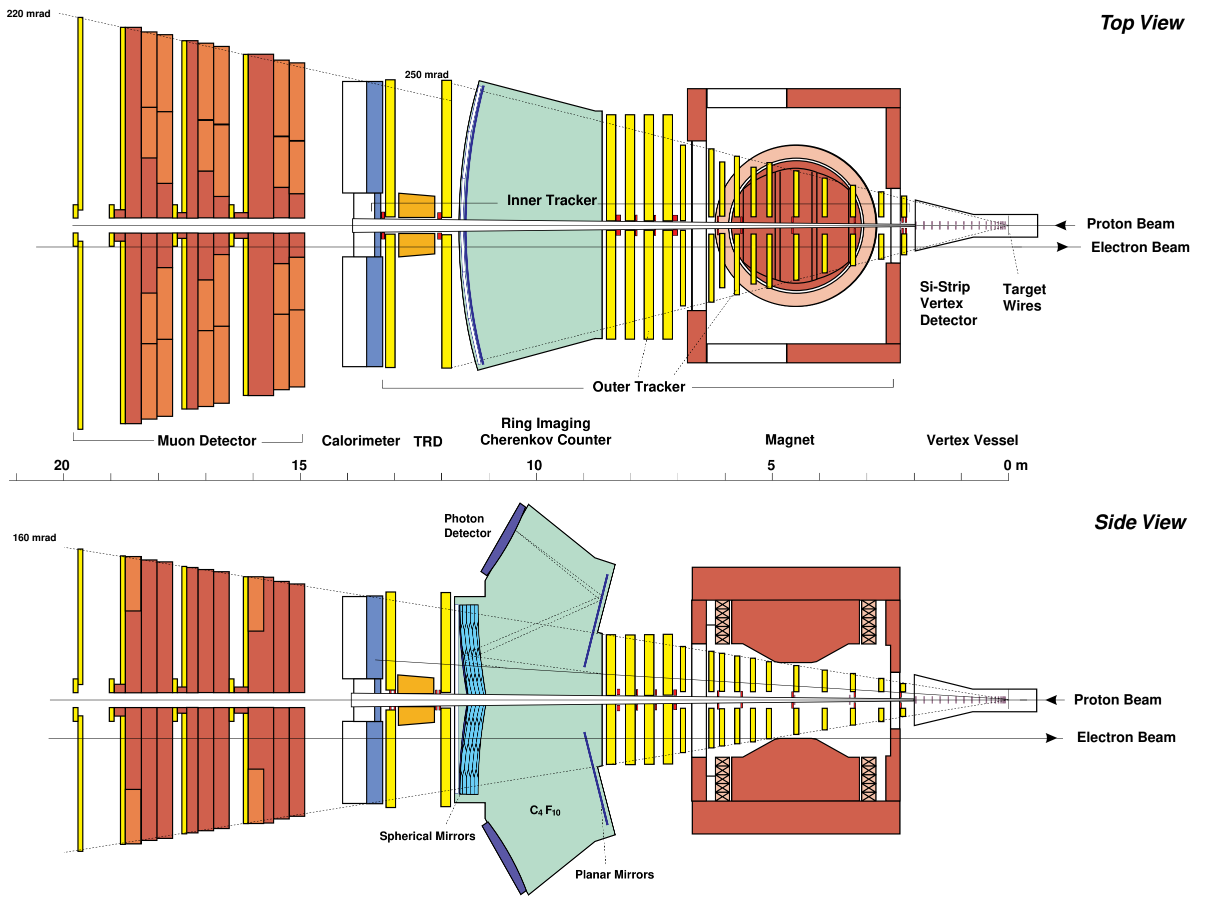

Figure 7. *The HERA-B spectrometer.*

tracking system, a ring imaging Cerenkov counter, an electromagnetic calorimeter, muon chambers and a trigger system.

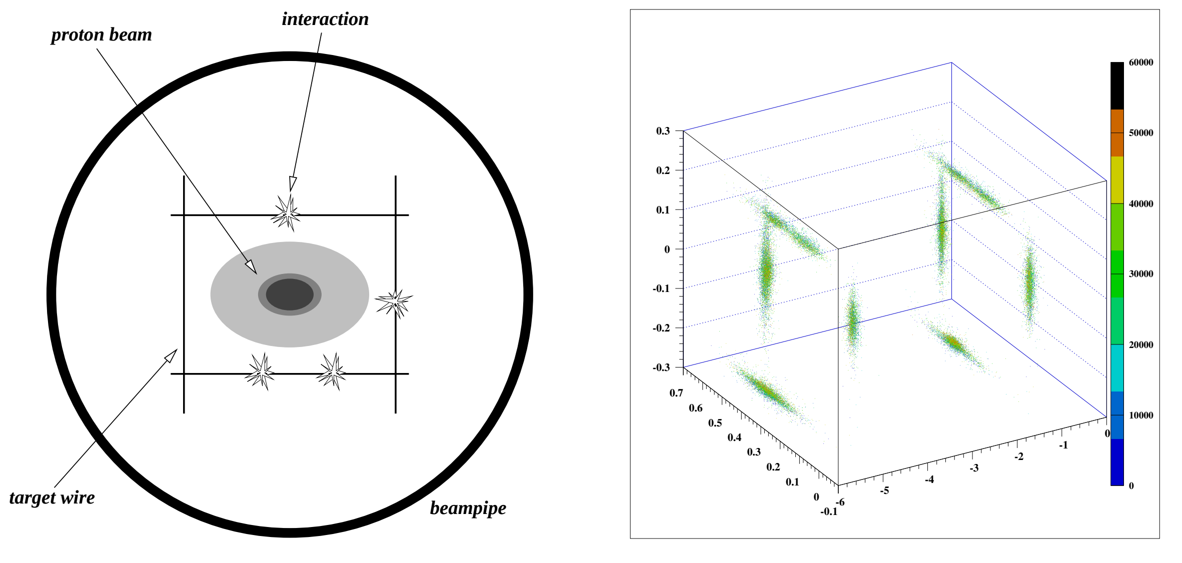

Figure 8. *HERA-B wire target concept (left), reconstructed vertex positions (right).*

HERA is a storage ring with proton and electron beams. The important requirement to HERA-B was not to interfere with HERA operation for *ep* collider experiments. The solution was to put several target wires in the halo of the proton beam. Protons which leave the core of the beam, and are anyhow lost for the beam, interact in wire targets (Ehret 2000) which consist of 8 wires organized in 2 stations (see Fig. 8). In this way an efficient separation of primary vertices for events with multiple interactions can be reached. The interaction rate can be changed by moving the wire targets. They are retractable, so the number of wires in operation can vary from 1 to 8. Operation of the wire target is very stable and meets the criteria of small interference with the storage ring.

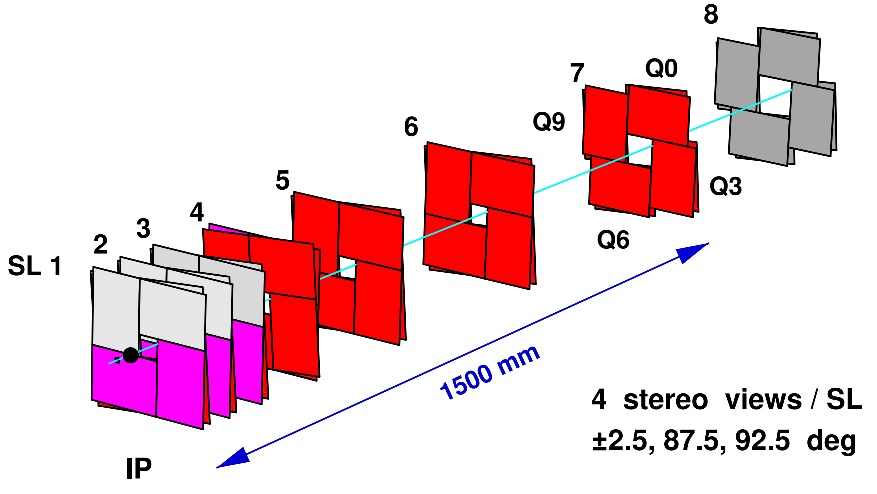

Figure 9. *The HERA-B vertex detector system.*

The purpose of the vertex detector system (VDS) is to provide track co-ordinates for reconstructing decay vertices and the impact parameters of decay products. The VDS (Masciocchi 2001) consists of 64 double–sided silicon microstrip detectors which are structured in eight super–layers of four quadrants around the proton beam axis (Fig. 9). To minimize multiple scattering, the first seven super–layers are organized in a Roman pot configuration. The VDS has been successfully operated for several years with interaction rates up to 40 MHz.

The tracking system comprises detector elements which are organized in superlayers around the proton beam pipe. The tracking super–layers extend over a length of 11 m. The first group of super–layers is situated inside the magnetic field of a dipole magnet, while the others are in the field–free region. In accordance with the increasing particle flux towards small polar angles, the system is divided in two parts consisting of detector elements with different granularity: outer tracker and inner tracker. The Outer Tracker (OTR) is the main part of the tracking system. It measures charged tracks in almost the whole geometrical acceptance. It consists of honeycomb drift chambers of two different granularities (Fig. 10), covering in total an area of about 1000 m^2. The system has to operate in a high radiation environment, so that several serious aging problems had to be solved (Hohlmann 2001). During the year 2000 run, the overall hit efficiency was somewhat worse than expected, mainly due to HV failures of individual wires. The error could be traced, and was repaired after the end of the run period. We note that the HERA-B outer tracking system is the first large area detector working in a LHC–like environment.

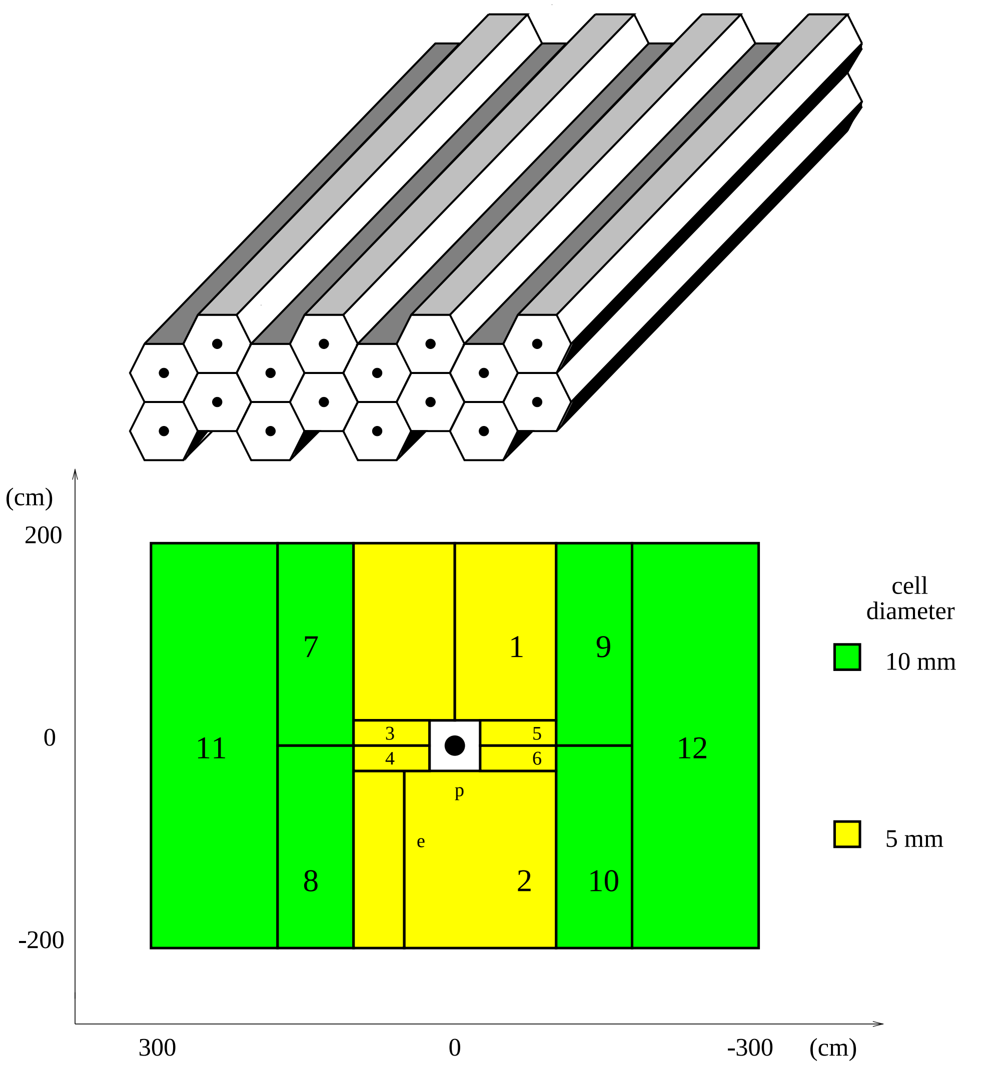

Figure 10. *The HERA-B Outer Tracking system: honeycomb drift chambers (top), modular structure (bottom).*

The inner tracker (ITR) measures tracks at small distances from the beam, and provides input for the first level trigger (Gradl 2001). The ITR elements cover the region from 6 cm to 25 cm around the beam pipe, with particle flux that can reach 10^6 per square centimeter per second. The detectors use micro strip gas chambers with a gas electron multiplier stage (GEM), as shown in Fig. 11. In the 2000 year run, the operation of the ITR was stable after an extensive conditioning phase, with performance close to the design value. Performances of the complete tracking system are reflected in Fig. 12 where distributions of invariant masses of K^0_S and Λ candidates, calculated from reconstructed tracks are shown. Selection involved vertex and tracking detectors only.

The purpose of the ring imaging Čerenkov counter (RICH) (Ariño et al. 2000) is the identification of charged hadrons. Charged particles radiate Čerenkov photons in the gaseous C_4F_{10} radiator. Photons are reflected from two systems of mirrors and collected on photon detectors where they form rings. The photon detectors consist of pads, based on multianode photomultipliers with a lens based light collection (Broemmelsiek 1998) system as shown in Fig. 14. To match the variation in occupancy and reduce the cost, two

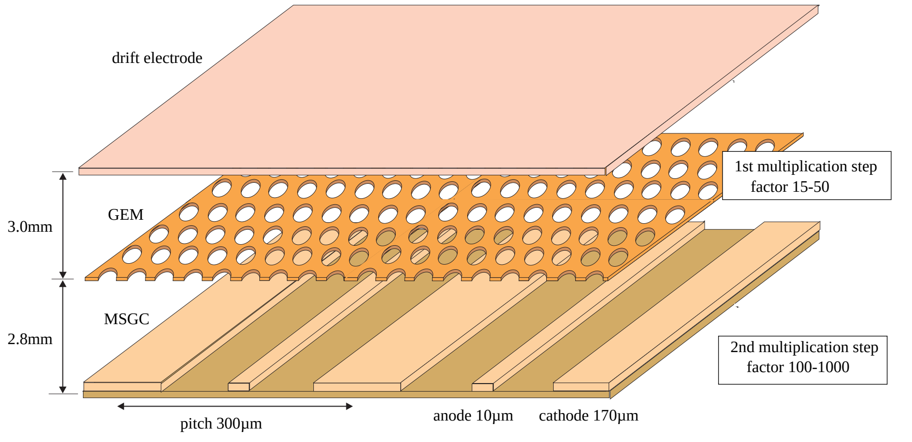

Figure 11. *MSGC-GEM detector structure.*

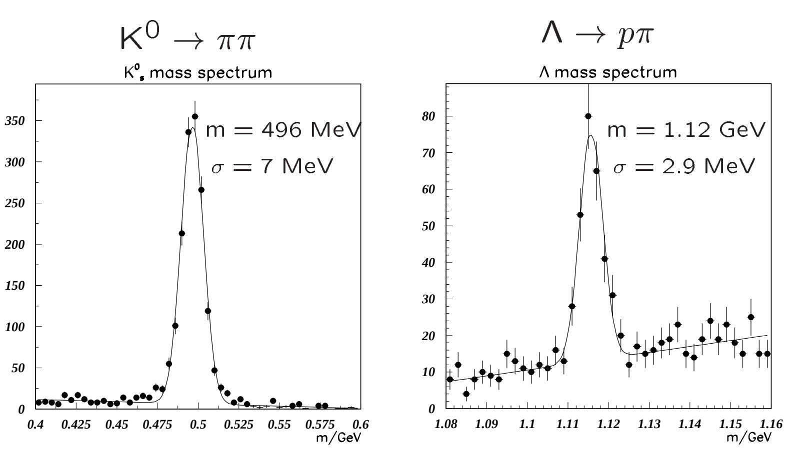

Figure 12. *Performance of the HERA-B tracking system: the K^0_S and Λ signal*

multianode PMT types are employed, 16 and 4 channel versions of the Hamamatsu R5900 tube. The system which has to stand typical rates of 1 MHz per channel in the hottest parts, has been in operation since summer 1998, with very few noisy ($< 0.2\%$) or dead channels (Fig. 15). For ultrarelativistic particles, the average number of photons in a ring is 32. Also, the single photon resolution ($\sigma_\theta^{RICH} = 0.7$ mrad for the finer, 1 mrad for the coarser granularity region) is in excellent agreement with the design value. Capabilities of the RICH for particle identification are concluded from the measured data. Fig. 16 shows the probability that a muon from a J/ψ decay is recognized as a muon by the RICH, as a function of muon momentum. The performance of RICH is expected to improve even further with the progress in alignment of the tracking system.

The electromagnetic calorimeter (Avoni et al. 2001) measures the photon energy, discriminates hadrons against electrons and gives an electron pretrigger. The calorimeter is of the "shashlik"-type with three different granularities in order to match occupancies. The measured energy resolution, ($\frac{\sigma(E)}{E} = 1.7\% \oplus \frac{22.5\%}{\sqrt{E}}$), is close to the design value.

The purpose of the muon detector (V. Eiges et al. 2001) is to separate muons from

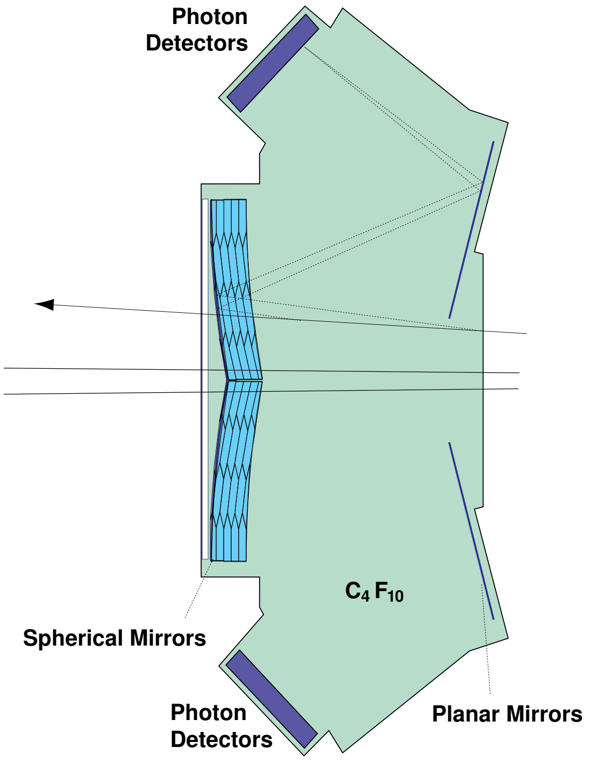

Figure 13. *Layout of the HERA-B RICH.*

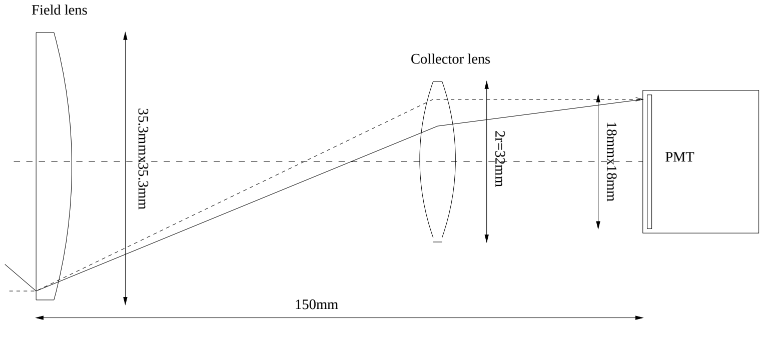

Figure 14. *Light collection system for each PMT of the HERA-B RICH photon detector.*

hadrons and to give a muon pretrigger. It consists of four layers of detector elements embedded in iron absorbers. Three types of detector elements (tube, pad and pixel chambers) are used in order to match the required granularity. In the 2000 run, the muon pretrigger provided a good J/ψ signal. Since the pretrigger requires a fourfold coincidence of signals in the pad chambers, its performance was limited by inefficiencies found in certain areas of chambers.

The huge background of inelastic proton-nucleon scattering above the signal requires a highly selective and efficient trigger. The main idea of the HERA-B trigger (Gerndt 2000, Kreuzer 2001) is to search for a pair of high-pt leptons, with the invariant mass consistent with the J/ψ mass. At the pretrigger level regions of interest are defined in the detector which correspond to particles with high transverse momentum. The pretrigger uses data from the calorimeter, the muon and the tracking systems. The first level trigger performs pattern recognition in the tracking system, reconstructs tracks and performs a cut on

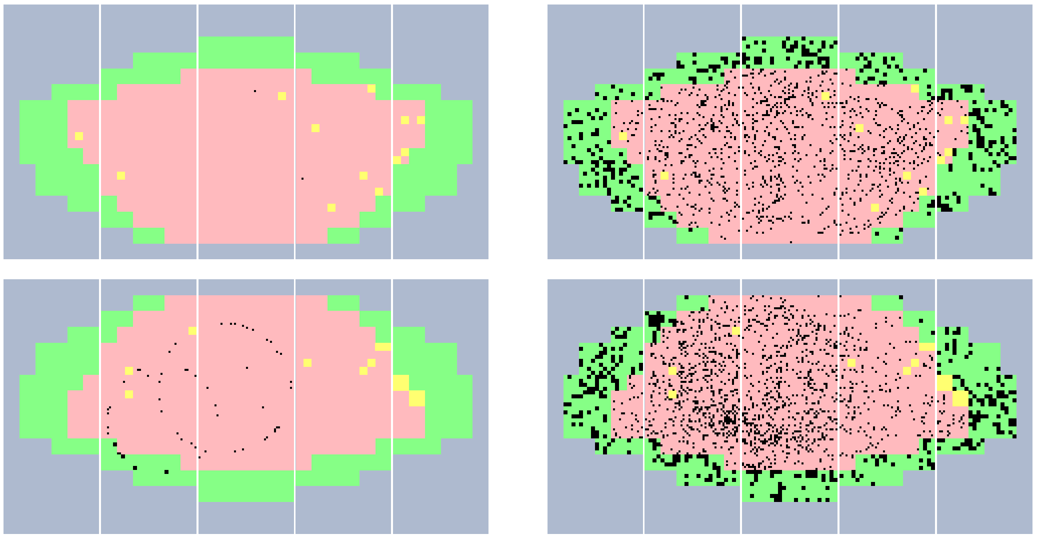

Figure 15. *HERA-B RICH: a low occupancy background event with two rings on the photon detector (left), a typical event (right).*

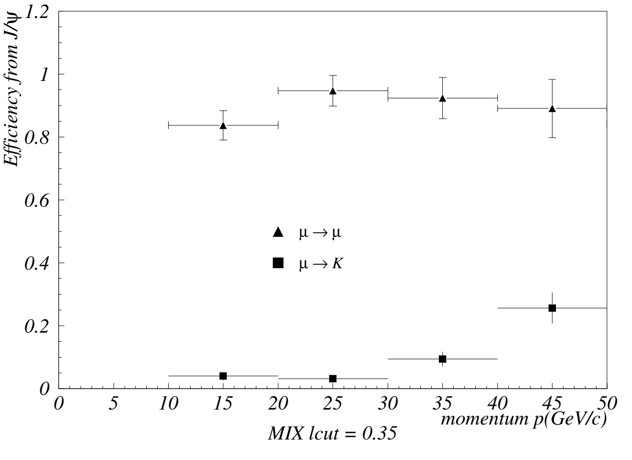

Figure 16. *HERA-B RICH: particle identification efficiency as determined from $J/\psi \to \mu\mu$ decays.*

the invariant mass of the candidate pairs. The track reconstruction is performed with dedicated processors along the tracking system stations (Fig. 17), by starting from the track candidate as defined by the pretrigger system. The rate reduction of the first trigger level is designed to be 200. The second and third level trigger refine track candidates and search for vertices. Their designed suppression factors are 100 and 10, respectively. The forth level trigger performs the complete event reconstruction and writes data to storage. The best results of the trigger in the 2000 run were achieved with the first level trigger requirement of a single high-pt lepton, while a search for the second high-pt lepton was performed in the second level trigger. We note, however, that in this initial run period the first level trigger efficiency was much below the design value (e.g. 20% for single muons, 54% for single electrons, instead of 90%), mainly due to inefficiencies in tracking and muon chambers.

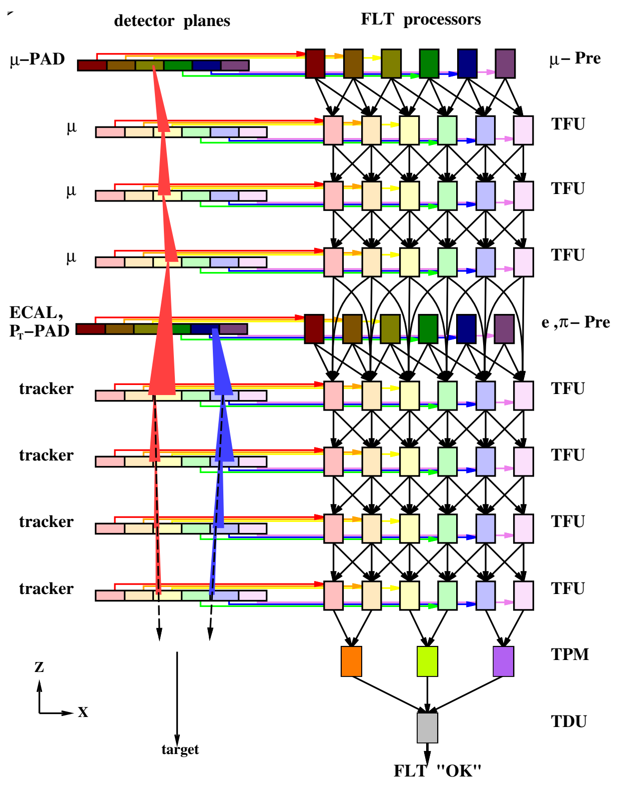

Figure 17. *HERA-B first level trigger system: pretrigger defined candidates are followed trough track finding units (TFU), and combined to pairs in the track parameter unit (TPM); the final decision is taken by the trigger decision unit (TDU).*

3.2 HERA-B status and plans

The experiment was approved in 1995. The design and construction of detector elements that can cope with extremely high fluxes were a technological challenge. Problems with the tracking system caused a substantial delay in the time schedule of HERA-B. The installation of the full detector was completed in February 2000. The first phase of commissioning lasted 6 months, until the HERA shutdown in August 2000 (HERA-B Collaboration 2000). The end of shutdown, and accordingly continuation of operation of HERA-B is expected in the second half of 2001.

Due to the late start of operation, HERA-B is not competitive in measurement of CP violation. In the 2001/2002 running period the experiment will concentrate on measurements of reactions which contain a J/ψ meson, for which the detector is optimized. Based on the results of the 2000 run and on the achieved detector improvements, it is expected that for the next run 1500 reconstructed J/ψ events will be collected per hour, resulting in about 2.1 million event in the full running period, altogether half a year. With these data HERA-B can make important contributions to two topics: measurement of nuclear dependence of charmonium production and measurement of the $b\bar{b}$ cross-section.

A suppression of the yield per nucleon of heavy vector mesons in proton-nucleus, pion-nucleus, and heavy ion collisions is observed in heavy nuclei compared to light nuclei, $\sigma = \sigma_n A^\alpha, \quad \alpha < 1$ (Leitch et al. 2000, Alde et al. 1991, Leitch et al. 1995). It is found that α strongly depends on x_F and p_T of the produced vector meson, and that ψ' is more suppressed than J/ψ. Various mechanisms can contribute to the suppression.

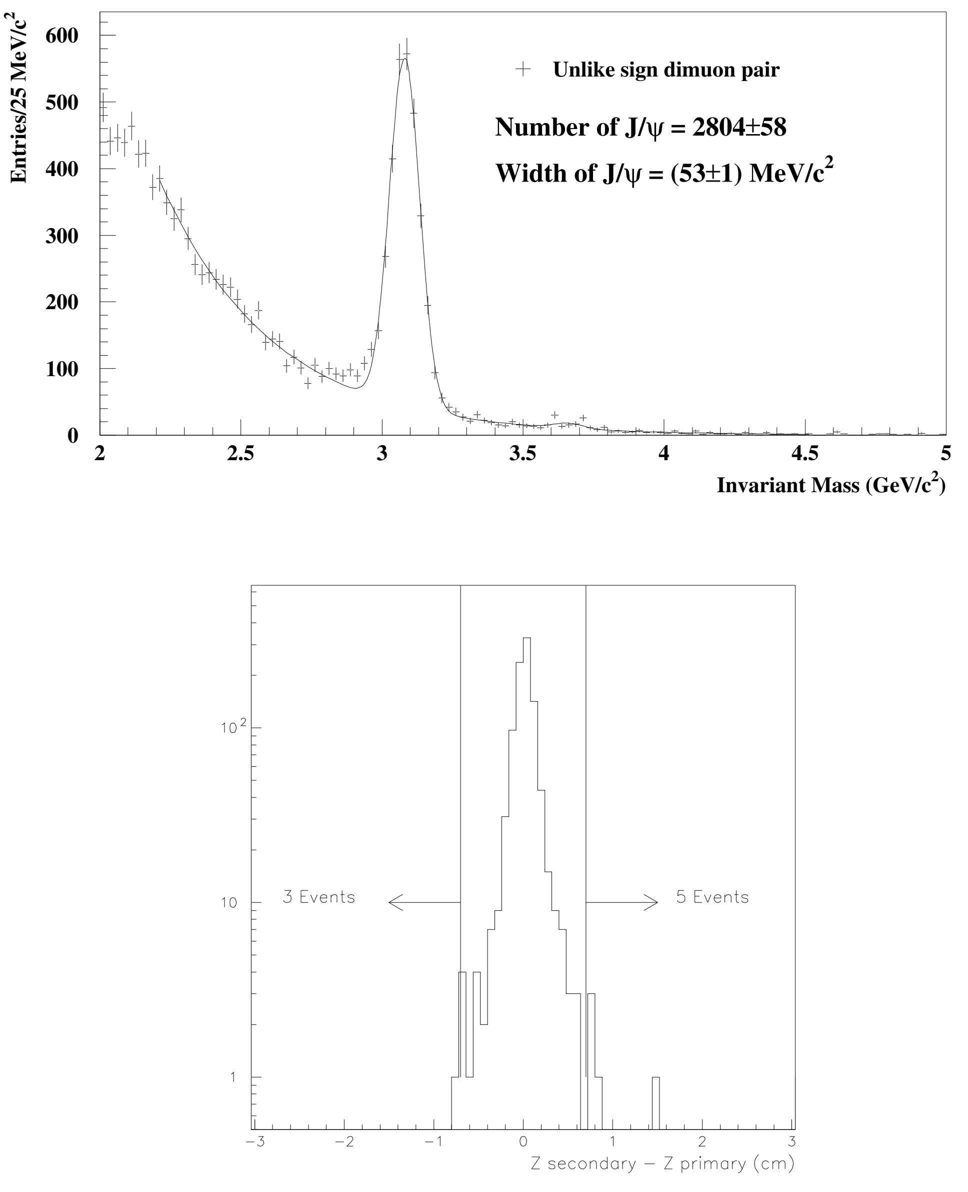

Figure 18. *HERA-B performance: di–muon invariant mass spectrum (top), decay length distributions in J/ψ mass region (bottom).*

Their relative importance is still not clear. HERA-B has several advantages compared to the existing measurements. It can measure the production of J/ψ mesons with x_F as low as -0.4, while the existing data are restricted to $x_F > -0.1$. Another advantage is that HERA-B has an electromagnetic calorimeter, which enables a measurement of the suppression of χ_c production using the $J/\psi\gamma$ decay mode. Also, HERA-B can simultaneously run with target wires made of different materials, thus reducing the systematical error from time dependent detector inefficiencies. Last year HERA-B took data using Ti and C wires. The result $\alpha = 1.027 \pm 0.043(stat)$ has low accuracy due to small statistics. For the the next run, a statistical error on α of a few per mills is expected for every x_F bin of 0.05 width. The corresponding error for ψ' will be approximately 1%. The systematical error on α will be or order of 2% for J/ψ and somewhat larger for ψ'. It will mainly come from the determination of the ratio of luminosities seen by a certain wire.

The other interesting research topic for the 2001/2002 run is the measurement of $\sigma_{b\bar{b}}$. In the relevant kinematic region, there are two measurements with inconsistent results (Jansen et al. 1995, Alexopoulos et al. 1999). Moreover, in the related processes, $\pi A \to b\bar{b}X$, experimental studies showed that the theoretical predictions have considerably underestimated the cross section. The measurement of $\sigma_{b\bar{b}}$ at HERA-B will be based on a comparison of inclusive $b \to J/\psi X$ with direct J/ψ production. The J/ψ candidates with decay vertices away from the target wire will be attributed to decays of b hadrons. In the next running period it is expected that about 340 events of this type will survive all cuts with a small background. The resulting $\sigma_{b\bar{b}}$ is expected to have a statistical accuracy of about $5-10\%$. The systematical error will be due to the b decay model ($< 8\%$) and also to the experimental error on $\sigma_{pA\to J/\psi X}$.

To summarize, we first note that HERA-B is the first experiment working in a LHC-like environment, such that the experience accumulated during the construction and commissioning is vital for the success of the next generation of hadron experiments. The main goals of HERA-B for the period 2001/2002 are the upgrade and repair during the 2001 shut–down, final commissioning of the detector, and measurement of the nuclear dependence of charmonium production and $b\bar{b}$ production cross section.

4 BTeV - a second generation B factory

The motivation for the BTeV experiment relies on the expectation that in the next few years the e^+e^- B-factories will firmly establish the evidence for CP violation in B decays, but that several questions will remain open due to lack of statistics, as well as due to the restricted set of available final states. The goal of BTeV is therefore to perform high precision measurements of CP parameters γ, α, χ, in decays of B^0, $B^\pm$, B_s mesons, as well as searches for new physics in rare and FCNC decays (Stone 2001).

The experiment (Santoro 1997, Skwarnicki 2001) will exploit the very large production cross section for $b\bar{b}$ pairs in the forward and backward direction in $p\bar{p}$ collision at Tevatron (Stone 1997). Moreover, the boost factor $\beta\gamma$ becomes very large outside the region occupied by central collider detectors CDF and D0 ($|\eta| < 2$, see Fig. 2). As can be seen from Fig. 19, pairs are produced either both in the forward or both in the backward direction, such that a single arm spectrometer similar to HERA-B would in principle be sufficient.

4.1 BTeV spectrometer

To accomplish its goals, the BTeV spectrometer (Sheldon 2001), shown in Fig. 20, has to meet the following requirements. It has to be able to efficiently trigger on hadronic B decays. It also needs a high resolution vertex detector for the measurement of B_s oscillations, an excellent PID system for π/K separation and a high resolution electromagnetic calorimeter for π^0 reconstruction. Needless to add that its components have to survive high interaction rates. Finally, it needs a high capacity DAQ system for a large number of read-out channels.

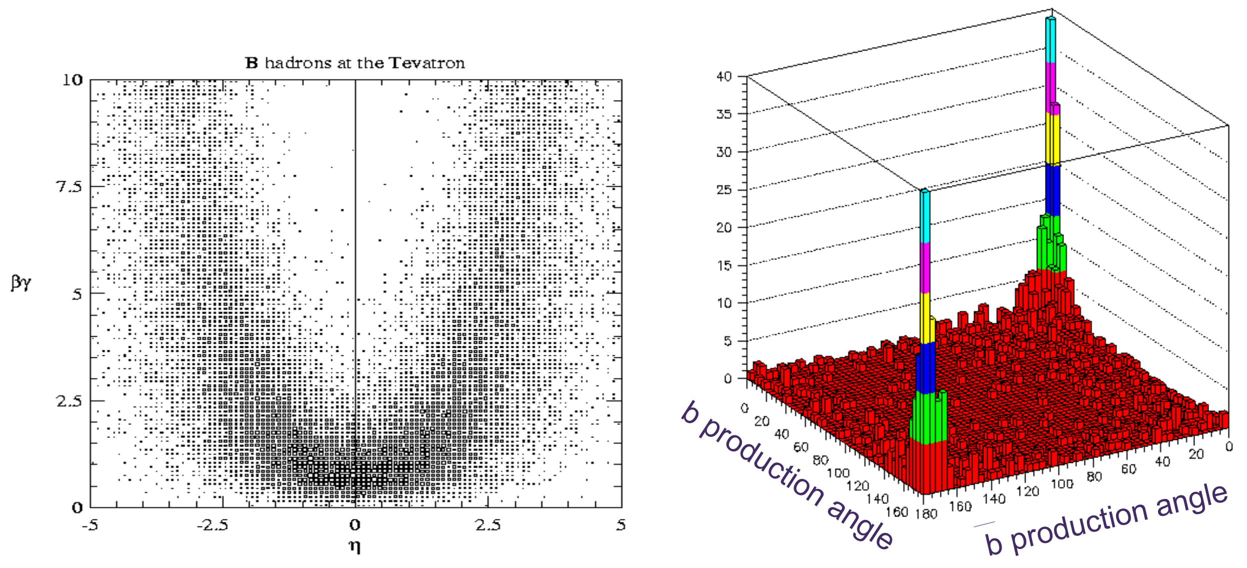

Figure 19. *Production of $b\bar{b}$ pairs at BTeV: dependence of boost on the pseudorapidity (left), correlation of production angles of the $b\bar{b}$ pair (right).*

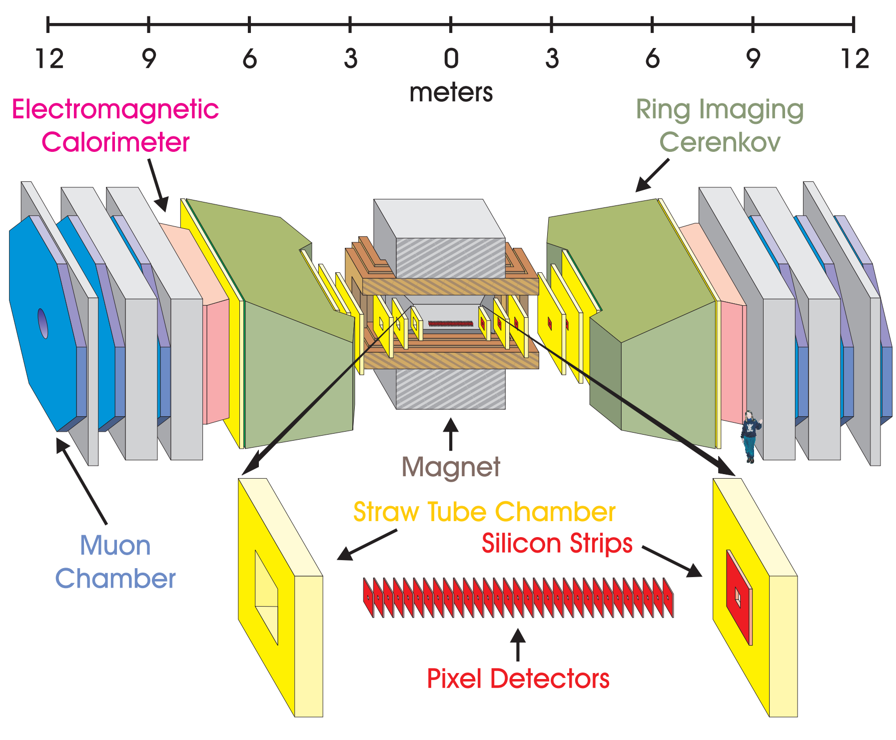

Figure 20. *BTeV spectrometer layout with an expanded view of the counters in the interaction region.*

The BTeV tracking system has three major parts, a vertex pixel detector, a system of straw-tube chambers as the main tracking device, and silicon strip detectors for tracking in the vicinity of the beam pipe. The pixel detectors are one of the core subsystems of the spectrometer (Artuso 2001). Their use is essential to eliminate ambiguities in the high track density region. In addition, they provide the detached vertex trigger. The expected advantage of such a detector is a low noise performance. The employed read-out electronics, which is in such a device subject to the same radiation load as the detector, was proven to be radiation hard due to the deep sub-micron process used (Christian 2001).

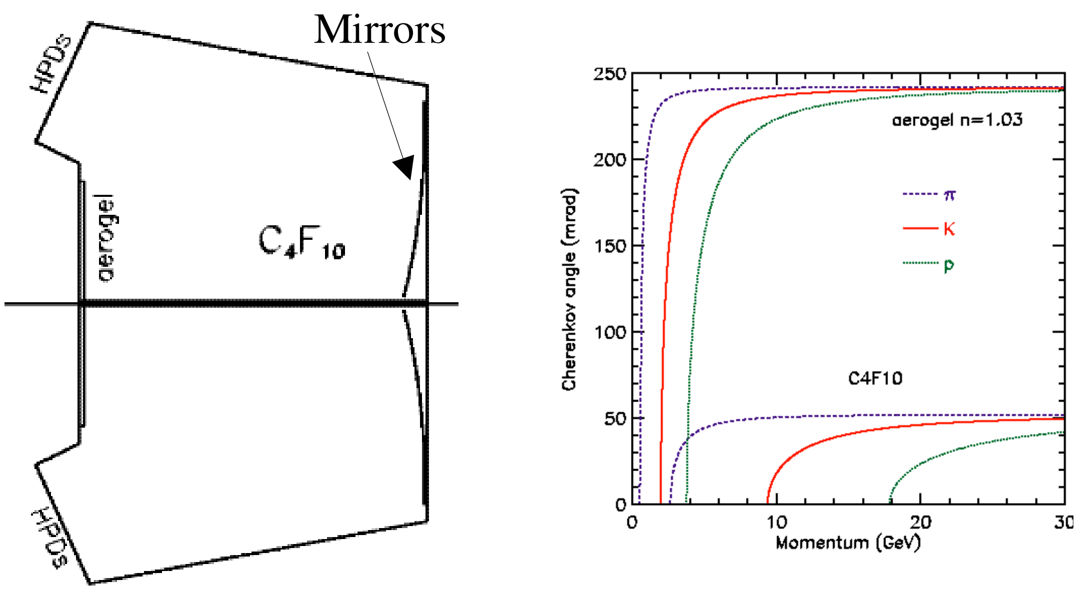

Figure 21. *BTEV RICH: detector layout with aerogel and C_4F_{10} radiators, spherical mirrors and HPD photon detectors (left), momentum dependence of the Čerenkov angle in the two radiators (right).*

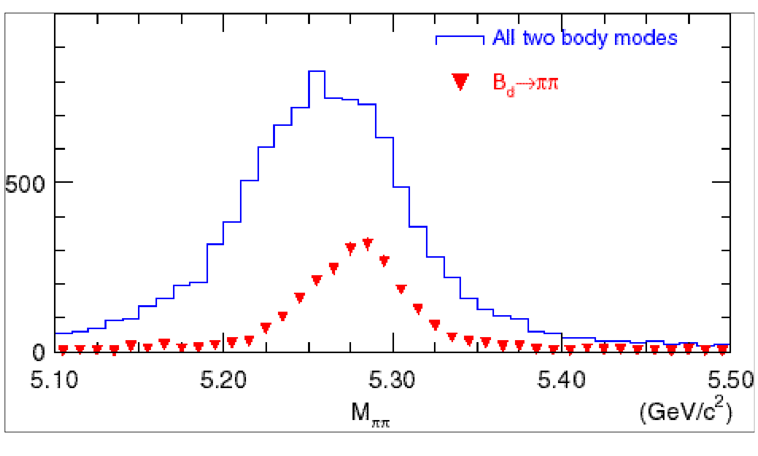

Figure 22. *Invariant mass distributions as determined by MC simulation for the $B \to \pi^+\pi^-$ decay together with the two body background sources, $B \to K\pi$, $B_s \to KK$ and $B_s \to K\pi$, without particle identification criteria.*

To cover the π/K separation over the interval $3 < p < 70$ GeV/c, a RICH counter (Fig. 21) with the same radiator gas, C_4F_{10}, as in the case of HERA-B will be used. To supplement the performance in the low momentum region and to improve the p/K separation, plans are discussed to add an aerogel radiator. The identification of hadrons is essential for both the tagging of b-flavour in CP violation and mixing measurements,

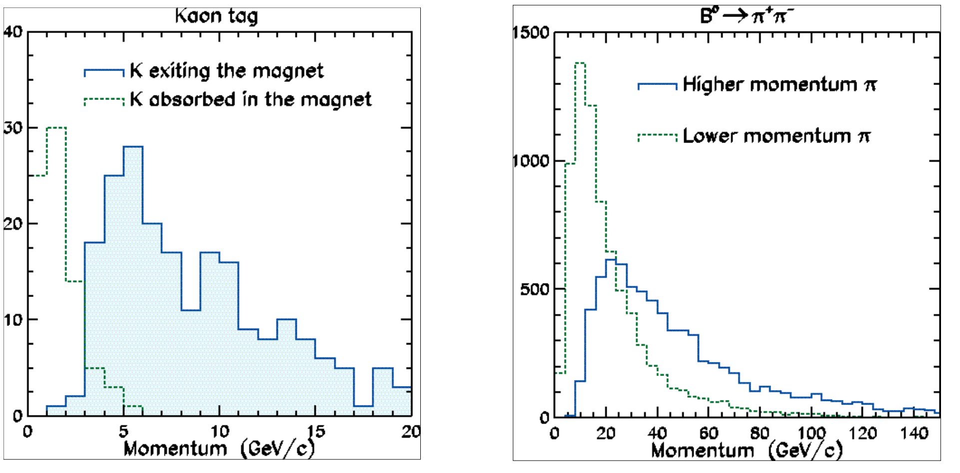

Figure 23. *Momentum spectra of tagging kaons (left) and pions from $B \to \pi^+\pi^-$ (right).*

as well as for the identification of particles in hadronic final states, e.g. $B \to \pi^+\pi^-$. The importance of the latter is illustrated in Fig. 22, where the $B \to \pi^+\pi^-$ events are obscured by a large background from other, kinematically similar, two-body decays. The corresponding kaon and pion momentum interval the identification device has to cover, can be deduced from in Fig. 23. Unlike HERA-B, a novel type of a position sensitive photon counter will be used, the hybrid photon detector (HPD) (Alemi 2000). The detector, shown in Fig. 24, uses a high electric field to accelerate photo-electrons which are, in turn, detected in a silicon pixel detector. The photon detector is of the same type as the one envisaged for LHCb (Wotton 2000), and is still under development.

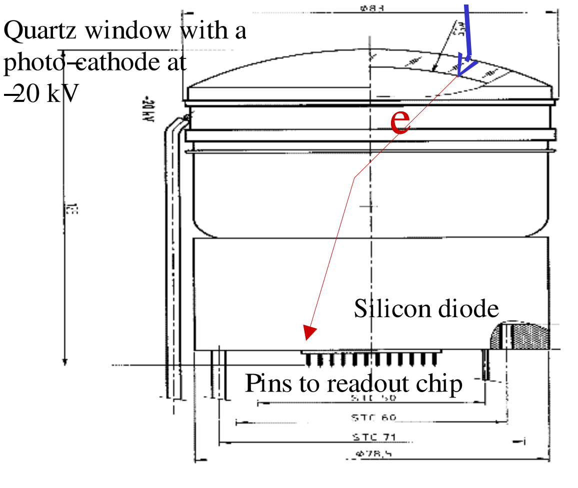

Figure 24. *The photon detector of the BTeV RICH counter, a hybrid photo detector (HPD).*

For the calorimeter which should allow for high resolution and radiation tolerance, the same type of crystals, $PbWO_4$, will be used as in the CMS experiment. The CMS technology will be used for the production of 22000 pieces of 27x27x2220 mm^3 size. The crystals are radiation hard, fast scintillators with 99% of light emitted in less than 100 ns, and will be read-out with PMTs. The energy resolution as expected from a full

GEANT simulation amounts to $\frac{\sigma(E)}{E} = 0.55\% \oplus \frac{1.6\%}{\sqrt{E}/\mathrm{GeV}}$, and the position resolution is $\sigma_x = \frac{3500\mu\mathrm{m}}{E/\mathrm{GeV}} \oplus 200\mu\mathrm{m}$.

The muon detector will be used both to identify muons, as well as to provide an auxiliary di-muon trigger for checks of the detached vertex trigger, in particular in the commissioning phase. It consists of two toroids with three detector sets.

One of the main components of the BTeV spectrometer is the trigger system, in particular the its first level (Artuso 2001). It is meant to find segments in the entrance and exit of the pixel detector as shown in Fig. 25. It will then match segments, get crude momentum estimates, and reject low momentum tracks from further use for vertex determination. In the next step, the primary vertex will be found, and for each of the tracks which miss it, the significance of detachment, $b/\sigma(b)$, will be calculated (Fig. 26). The goal of the this first trigger level is a factor 100 or more rejection of crossings

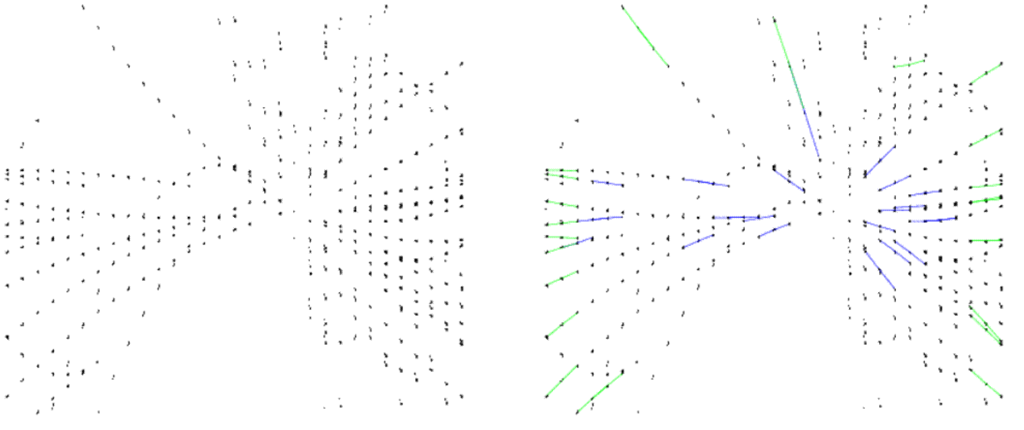

Figure 25. *Event in the pixel detector, with the horizontal coordinate compressed by factor 10. Left: raw event, right: segments found at the entrance and exit of the detector.*

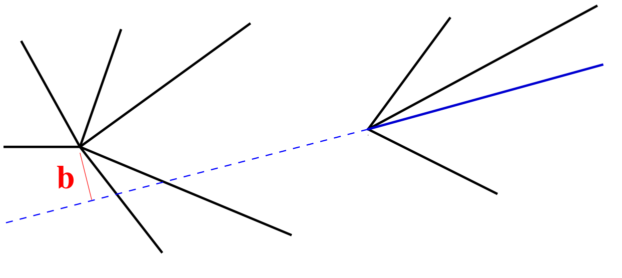

Figure 26. *Detachment b from the primary vertex is calculated for each individual track.*

without a $b\bar{b}$ pair, and an efficiency exceeding 50% for interesting events. As an example, a requirement of two tracks with $b/\sigma(b) > 6$ leaves 1% of beam crossings, and has 63% efficiency for $B^0 \to \pi^+\pi^-$, 70% for $B^- \to D^0 K^-$, 50% for $B^0 \to J/\psi K_S^0$. The dependence of signal efficiency and background rejection power on the detachment cut for different number of tracks is shown in Fig. 27.

The second trigger level will rely on refitted pixel segments, include more hits, link tracks to downstream tracker (straws and strips) for accurate momentum measurement, and redo the fit for a better detachment determination, with a rejection of factor of 10 or

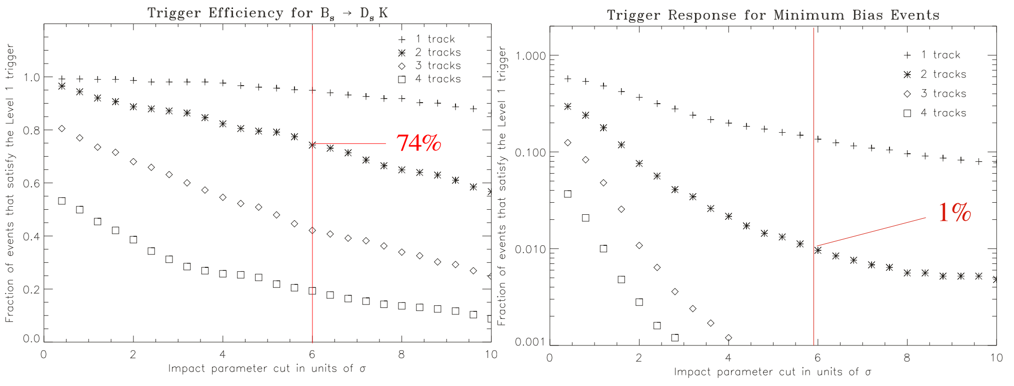

Figure 27. *Level 1 trigger efficiency for $B_s \to D_s K$ (left) compared to the efficiency for minimum bias events (right), as determined from MC studies.*

Mode	e^+e^- B-factories with 500 fb^{-1}	BTeV yield in 10^7 s
$B_d \to \pi^+\pi^-$	850	24000
$B_d \to \phi K^-$	700	11000
$B_d \to \phi K_S$	250 (75 tagged)	2000 (200 tagged)
$B_d \to K^*\mu\mu$	50	2200
$B_s \to J/\psi\eta^{(\prime)}$	-	15000

Table 2. *Comparison of expected BTeV yield of reconstructed events in some interesting decay modes with the expectations from the data collected at the e^+e^- B-factories by the year 2005.*

more at 90% efficiency. The third level will involve more processing, with the goal of an event output rate of 4 kHz, each of 40 kbyte size.

4.2 BTeV physics reach

The examples shown in the comparison table, Tab. 2, are meant to illustrate in which respect the BTeV experiment is a second generation B-factory. In the first column we list the expected number of events as collected by the B-factories with integrated luminosity of 500 fb^{-1} (as expected around 2005). In the second column we present the amount of data the BTeV experiment is expected to reconstruct in one effective year (10^7 s). The interested reader is refered to an excellent review of the experiment, and its comparison to the LHCb experiment (Stone 1997).

5 Summary

We summarize this overview by observing that the hadron production of B mesons has a large cross section. However, background levels are high, such that elaborate triggering is needed to extract the signal events. In addition, a high rate operation of the detector is required over extended run periods. The results of B physics studies by the CDF experiment prove that B physics can be done at hadron machines. The HERA-B spectrometer components are ready after an extensive radiation hardness and high rate tolerance R&D and a commissioning phase. The trigger of the HERA-B spectrometer is being commissioned, and a year of data taking expected in 2002 will add to the valuable experience for the next generation of experiments at hadron machines. Finally, the second generation of B factories, BTeV and LHCb, is under construction, and is expected to open a new B physics era around the year 2005.

Acknowledgments

I thank K Pitts and M Schmidt for providing me with relevant information on the B physics results, upgrade and expected reach of the CDF experiment, and S Stone for useful discussions on the BTeV project. I congratulate my colleagues from HERA-B for their heroic efforts in mastering a very difficult experiment.

Last but not least, I would like to thank the organizers of the School for their hospitality, and congratulate them for the excellent scientific and social program.

References

F. Abe *et al.* [CDF Collaboration], 1988, *Nucl. Instrum. Meth.* **271** 387.
T. Affolder *et al.* [CDF Collaboration], 1999, *Phys. Rev. Lett.* **83** 3378.
T. Affolder *et al.* [CDF Collaboration], 2000, *Phys. Rev.* **D61** 072005.
T. Affolder *et al.* [CDF Collaboration], 2000a, *Phys. Rev. Lett.* **85** 4668.
D.M. Alde *et al.*, *Phys. Rev. Lett.* **66** 133.
M. Alemi *et al.* [TA2 Collaboration], 2000, *Nucl. Instrum. Meth. A* **449** 48.
T. Alexopoulos *et al.*, 1999, *Phys. Rev. Lett.* **82** 41.
I. Ariño *et al.*, 2001, *Nucl. Instrum. Meth. A* **453** 289.
M. Artuso [BTeV Collaboration], 2001, *Nucl. Instrum. Meth. A* **462** 249.
G. Avoni *et al.*, 2001, *Nucl. Instrum. Meth. A* **461** 332.
F. Bedeschi, 2001, *FERMILAB-CONF-01-006-E*
D. C. Christian *et al.*, 2001, *Nucl. Instrum. Meth. A* **473** 152.
K. Ehret, 2000, *Nucl. Instrum. Meth. A* **446** 198.
V. Eiges *et al.*, 2001, *Nucl. Instrum. Meth. A* **461** 104.
HERA-B Collaboration, 2000, *DESY-PRC* 00/04.
C. Gay, 2000, *Ann. Rev. Nucl. Part. Sci.* **50** 577, *hep-ex*/0103016.
W. Gradl, 2001, *Nucl. Instrum. Meth. A* **461** 80 2001.
B. K. Hall *et al.*, 2001, *FERMILAB-CONF-01-335.*
M. Hohlmann, 2001, *Nucl. Instrum. Meth. A* **461** 21.
D.M. Jansen *et al.*, 1995, *Phys. Rev. Lett.* **74** 3118.
P. Kreuzer, 2001, *Nucl. Instrum. Meth. A* **462** 212.

M.J. Leitch *et al.*, , *Phys. Rev. D* **84** 3526.
M.J. Leitch *et al.*, , *Phys. Rev. D* **52** 4251.
T. Lohse *et al.*, 1994, *DESY-PRC* 94/02.
S. Masciocchi, 2001, *Nucl. Instrum. Meth. A* **461** 220.
H. G. Moser and A. Roussarie, 1997, *Nucl. Instrum. Meth. A* **384** 491.
M. Paulini [CDF Collaboration], 1999, *Int. J. Mod. Phys. A* **14** 2791, *hep-ex*/9903002.
K. T. Pitts [CDF Collaboration], 2000, *hep-ex*/0102010.
A. Santoro *et al.*, 1997, *FERMILAB-FN-660.*
P.D. Sheldon [BTeV Collaboration], 2001, *Nucl. Instrum. Meth. A* **462** 291.
T. Skwarnicki [BTeV Collaboration], 2001, *Nucl. Instrum. Meth. A* **462** 227.
S. Stone, 2001, these proceedings.
S. Stone, 1997, *hep-ph*/9709500.
S. Stone, 2001, these proceedings.
M. Tanaka [BTeV Collaboration], 2001, *Nucl. Instrum. Meth. A* **462** 165.
S. A. Wotton [LHCb RICH Group Collaboration], 2000, *Nucl. Instrum. Meth. A* **453** 296.

Appendix: How to measure B_s mixing?

In order to observe mixing in the B_s system, we have to measure the probability that a B_s (at $t = 0$) turns into $\bar{B}_s$ at time t. For the measurement we therefore need a well defined final state with precisely measured vertex position and momentum, and a tag to determine the initial B_s flavour (B_s or $\bar{B}_s$ at $t = 0$). Clearly, the final state has to be flavour specific. Several decay channels have been considered and used for measurements: the semileptonic $\mu D_s \nu$, $D_s \to \phi\pi^+, K^+K_S, K^+K^*$ decay chain, the $J/\psi K^* \to \mu\mu K\pi$ channel, as well as hadronic decays $D_s^{(*)}\pi^+(\pi^+\pi^+\pi^-)$. For tagging of the initial B_s flavour, the charge of the kaon or lepton from the associated B decay are usually used.

In what follows, we will give a simplified picture of the dependence of the maximal mixing parameter x_s an experiment can measure, on the resolution and available statistics. The interested reader should consult the reference Moser & Roussarie 1997 for full derivation and details.

We first start with a hypothetical perfectly tagged case, and a B_s at t=0. The probability that this B_s meson decays as a $\bar{B}_s$ depends on the proper time t in the following way, $(1 - cos(x_s t/\tau) \exp{(-t/\tau)}$. Imperfect tagging and background reduce the amplitude of the cosine term by a factor known as dilution (D) such that

$$r(B_s \to \bar{B}_s) = e^{-t/\tau}(1 - Dcos(x_s t/\tau)).$$

For lepton tagged events the value of D is about 0.18 (Fig. 28).

The amplitude is then further reduced by the finite resolution in proper time t. In the limit of a very good resolution ($\sigma_t << x_s\tau$), a simple quantitative estimate of the effect can be made by observing that the amplitude is reduced by events moving from the 'up' side of the wave to the 'down' side, the effect being most important in an interval of order σ_t around the node of the oscillating term (Fig. 29). In this region the function is approximately linear, and the fraction of events (i.e. its integral) in this interval can be roughly estimated to $\frac{\sigma_t^2 x_s^2}{2\tau^2}$.

This clearly has to be regarded as the first term in an expansion. A proper derivation involves a convolution of the time evolution curve and the detector response, and the am-

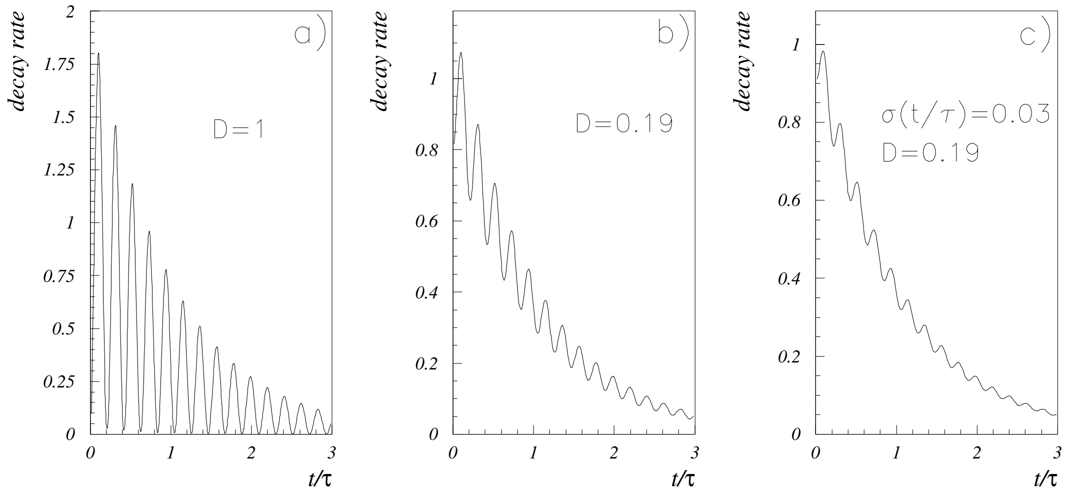

Figure 28. *B_s mixing: no dilution (a), the effect of dilution (b) and resolution (c) for the $x_s = 30$ ($\Delta m_s = 22 \quad ps^{-1}$) example.*

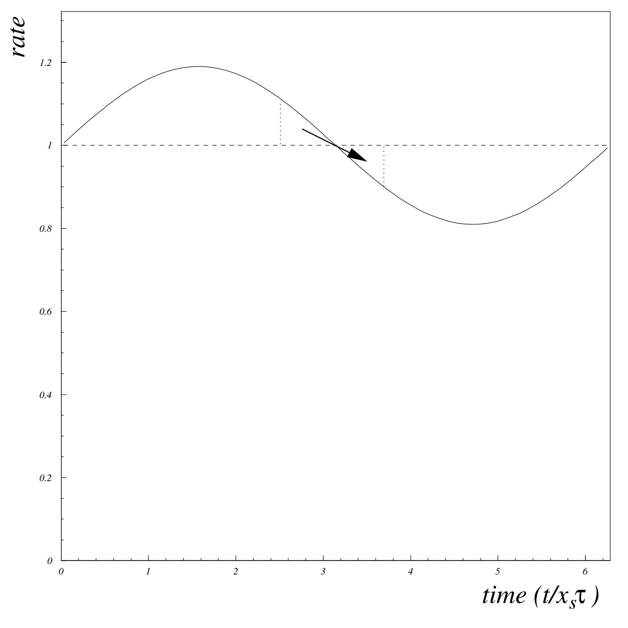

Figure 29. *Dilution of the oscillatory term due to finite resolution. The affected interval is indicated by dotted lines.*

plitude turns out to be reduced by a factor $e^{-\frac{\sigma_t^2 x_s^2}{2\tau^2}}$, in agreement with the rough estimate. As a result, we get a function of the form

$$e^{-t/\tau}(1 - D' cos(x_s t/\tau)),$$

shown in Fig. 28, with the dilution D replaced by $D' = De^{-\frac{\sigma_t^2 x_s^2}{2\tau^2}}$.

A simple estimate of the statistics required for a significant measurement can be made if we fix x_s, and divide the events in two classes, those from the 'up' part of the wave, and those from the 'down' part (Fig. 29). The measured oscillation amplitude for a given x_s differs from zero if the two classes are found to be differently populated. The distribution over the two classes is binomial, with probability for the 'up' part equal to $p = \frac{1}{2} + cD'$, where c is a constant of order 1. The error on p is in case we have made a measurement with N reconstructed and tagged events equal to $\sigma(p) = \sqrt{p(1-p)/N}$. This expression can be simplified for $p \approx \frac{1}{2}$ to $\sigma(p) \approx \frac{1}{2}\sqrt{1/N}$. The resulting error on the amplitude D' is $\sigma_{D'} \approx 1/(2c\sqrt{N})$, and the significance of the measurement equals to

$$D'/\sigma_{D'} \approx 2c\sqrt{N} D e^{-\frac{\sigma_t^2 x_s^2}{2\tau^2}}.$$

For a given required significance, the number of events needed, and thus the duration of the measurement, is proportional to $e^{\frac{\sigma_t^2 x_s^2}{2\tau^2}}$. This is a very steep function of the proper time resolution σ_t and the mixing parameter x_s, in particular in the region where the quadratic term in the exponent exceeds the value of 1. In the case of the upgraded CDF detector, where a σ_t of 45 fs is expected, this value is reached at $x_s = 30$.